British Journal of Mathematics & Computer Science
2(3): 137-150, 2012

SCIENCEDOMAIN *international*
www.sciencedomain.org

Biparameter Homotopy-based Direct Current Simulation of Multistable Circuits

H. Vazquez-Leal[*1], R. Castaneda-Sheissa[1], A. Yıldırım[2], Y. Khan[3], A. Sarmiento-Reyes[4], V. Jimenez-Fernandez[1], A.L. Herrera-May[5], U. Filobello-Nino[1], F. Rabago-Bernal[6], C. Hoyos-Reyes[1]

[1] *Electronic Instrumentation School, University of Veracruz, Xalapa, Veracruz, Mexico*
[2] *Department of Mathematics, Ege University, 4146 Sk. No. 16, Zeytinalani Mah. Urla-Izmir, Turkey.*
[3] *Department of Mathematics, Zhejiang University, Hangzhou 310027, China*
[4] *Electronics Department, National Institute for Astrophysics, Optics and Electronics, Sta. Maria Tonantzintla, Puebla, Mexico*
[5] *Micro and Nanotechnology Research Center, University of Veracruz, Boca del Rio, Veracruz, Mexico*
[6] *Physics Institute, Autonomous University of San Luis Potosi, San Luis Potosi, SLP, Mexico*

Research Article

Received: 22 March 2012
Accepted: 08 May 2012
Published: 13 October 2012

Abstract

The microelectronics area constantly demands better and improved circuit simulation tools. This is the reason that this article is to present a biparameter homotopy with automated stop criterion, which is applied to direct current simulation of multistable circuits. This homotopy possesses the following characteristics: symmetry axis, double bounding solution line, arbitrary initial and final points, and lessen the nonlinearities that exist in the circuit. Besides, this method will be exemplified and discussed by using a benchmark multistable circuit.

Keywords: Homotopy continuation; multistable circuit
2010 Mathematics Subject Classification: 53C25; 83C05; 57N16

1 Introduction

Solution to nonlinear algebraic equation systems (NAES) is needed for several areas of physics, particularly, in electronics where the solution of the equilibrium equation allows to study the direct current (DC) behaviour of integrated circuits before they are fabricated, allowing the designers to

**Corresponding author: E-mail: hvazquez@uv.mx*

optimize/redesign their circuits in order to achieve design specifications (Verhoeven et al., 2003). The most employed method to solve NAES is the Newton-Raphson (NR) method, which has quadratic convergence (Ogrodzki, 1994). However, homotopy continuation methods (HCM) (Wu, 2005; Wu, 2006a; Wu, 2006b; Varedi et al., 2009; Malinen and Tanskanen, 2010; Jalali et al., 2008; Di Rocco et al., 2011) have been proposed as an alternative because they have better convergence than the NR method. Likewise, the complexity of circuits have been continuously increasing, this translates in a greater probability of multiple operating points (Lagarias and Trajkovic, 1999; Goldgeisser and Green, 1998); this situation can be solved using HCM methods since they are capable to locate multiple solutions over one path, contrary to the NR method, it just can locate one solution per simulation.

Nevertheless, HCM methods (Vazquez-Leal et al., 2011a; Kuroki et al., 2007; Ma et al., 2002; Sarmiento et al., 2001) have some disadvantages, one of them is that in general they do not have a reliable stop criterion. It means that it is not possible to determine, with mathematical certainty, when to stop looking for new solutions on the homotopy path. In this sense, in Goldgeisser and Green (2005) a technique is proposed to restrict the search space for certain group of circuits including bipolar transistors, ensuring a stop criterion. Nevertheless, that homotopy requires advanced knowledge about multistable circuits to use it satisfactorily. Double bounded homotopy (DBH) (Vazquez-Leal et al., 2005b) and double bounded polynomial homotopy (DBPH) (Vazquez-Leal et al., 2011a) possess a formal stop criterion and can be applied to circuits containing diodes, tunnel diodes, BJT transistors, and MOS transistors, among others. Those kinds of homotopies are useful to simulate multistable circuits. Therefore, this work establishes a biparameter DBPH homotopy, which has the advantage of possess stop criterion and lessen nonlinearities present in the circuit.

This paper is organized as follows. In Section 2, we introduce the basic idea of HCM methods. In Section 3, we introduce the biparameter DBPH homotopy. For Section 4, a bipolar/diode circuit is solved using the proposed homotopy. In Section 5, we summarize our findings and suggest possible directions for future investigations. Finally, a brief conclusion is given in Section 6.

2 Basic idea of HCM methods

The equilibrium equation for any circuit can be formulated using the modified nodal analysis (MNA) (Ho et al., 1975) as initial step, it is defined as

$$f(x) = 0, \qquad f :\in \Re^n \to \Re^n, \tag{1}$$

where x represents the electrical variables of the circuit, and n the number of nodes plus the number of non-NA compatible elements.

Homotopy methods are based on the fact that solutions are connected by a curve, called "solution curve". To obtain this curve one additional parameter is added to the original equation system, it will help to obtain the following augmented equation

$$H(f(x), \lambda) = 0, \quad H :\in \Re^n \times \Re \to \Re^n, \tag{2}$$

where (H) represents the homotopy function, λ the continuation parameter, and $f(x)$ the original equation to be solved.

Thus, the original problem becomes a numerical continuation problem (Vazquez-Leal et al., 2011b, Vazquez-Leal et al., 2005a); where the continuation variable is the homotopy parameter λ. Therefore, $H(f(x), 0) = G(x)$, where $G :\in \Re^n \to \Re^n$ is a smooth map which has one trivial solution and $H(f(x), 1) = f(x)$, meaning that at $\lambda = 1$ the solution x_s for $f(x)$ is located.

3 Biparameter DBPH homotopy

Multiparameter homotopy adds more than one homotopy parameter to the equilibrium equation (Wolf and Sanders, 1996). Essentially, it has a similar behaviour to a uniparametric homotopy, because it has one trivial solution when the homotopy parameters has value of zero and the solution for $f(x)$ is located when the homotopy parameters reach the value of one. The multiparameter homotopy can be represented as

$$H(f(x), \lambda_1, \lambda_2, ..., \lambda_k) = 0, \tag{3}$$

where $\lambda_1, \lambda_2, ...\lambda_k \in [0, 1]$, k is the number of homotopy parameters, and x represents the nodal voltages and currents of the non-NA compatible elements (Ho et al., 1975).

On one hand, multiparameter homotopies (Wolf and Sanders, 1996) have been proposed to avoid fork bifurcations, singularities, among other problems that can be found on the homotopy paths. On the other hand, multiparameter homotopy applied to circuits can be interpreted as the nonlinear circuit deformation in a simplified circuit with trivial solution, such that when homotopy parameters are swept, the simplified circuit is transformed until it coincides with the original nonlinear circuit. Therefore, this type of homotopy produces a soft path to the solution. That circuital transformation is of broad interest since it is possible to create custom multiparameter homotopies to solve circuits characterized by specific nonlinearities like circuits composed of devices like: BJT/MOS transistors, memristors, and nanotubes, among others. Likewise, it is possible to apply one or more homotopy parameters embedded directly into the device model in order to linearise the circuit right at the beginning of the homotopy path; softly returning its original state (nonlinear) as the homotopy parameters reach the value of 1.

It is possible to formulate a biparameter homotopy with stop criterion using the double bounded polynomial homotopy (DBPH) (Vazquez-Leal et al., 2011a), its formulation is

$$H(f(x), \lambda) = (\lambda + a)\lambda(\lambda - a)(\lambda - 2a)(x - x_i)(x - x_f) + C(\lambda - a/2)^2 f(x)^2 = 0, \tag{4}$$

where λ is the homotopy parameter, a is a constant that represents the separation between solution lines $\lambda = 0$ and $\lambda = 1$, x_i is the initial point, x_f the final point, and C an arbitrary constant. Then, a second homotopy parameter is added; now, the homotopy is formulated as

$$\begin{aligned} H(f(x), \lambda_1, \lambda_2) = (\lambda_1 + a)\lambda_1(\lambda_1 - a)(\lambda_1 - 2a)(x - x_i)(x - x_f) \\ +C(\lambda_1 - a/2)^2 f(x, \lambda_2)^2 = 0, \end{aligned} \tag{5}$$

where $f(x, \lambda_2)$ represents the second homotopy parameter λ_2 embedded within the equilibrium equation $f(x)$.

The MNA method establishes a stimuli vector i_{est}; it contains the contribution of independent current sources, nonlinear resistors, among others. In a circuit containing bipolar transistors, the Ebers-Moll model contains diodes whose most simple model is a nonlinear current source that depends exponentially on the voltage drop in the diode. Therefore, the contribution of the nonlinear current source to the equation will be placed directly in the stimulus vector i_{est}.

The addition of the homotopy parameter into the equilibrium equation should be done in such a way that the homotopy path follows a path as soft as possible; this can be achieved multiplying λ_2 by the nonlinear stimulus vector ($\lambda_2 i_{est}$). This is done to suppress nonlinearities and energy sources of the circuit just at $\lambda_2 = 0$.

The biparameter homotopy can be expressed in general way as (using $a = 1$)

$$H(f(x), \lambda_1, \lambda_2 i_{est}) = \begin{cases} f(x_s) = 0 & \text{for } \lambda_1 = 1, \lambda_2 = 1 \text{ and } x = x^* \\ (x - x_i)(x - x_f) = 0 & \text{for } \lambda_1 = 0.5 \text{ and } \lambda_2 = 0 \\ f(x_s) = 0 & \text{for } \lambda_1 = 0, \lambda_2 = 1 \text{ and } x = x^* \end{cases}$$

where x_s represents the operating point of the circuit.

The λ_1 parameter is employed for the basic DBPH homotopy formulation and λ_2 parameter is embedded in the equilibrium equation in such a way that DBPH properties are preserved (Vazquez-Leal et al., 2011a), among of them we can mention: symmetrical branches, symmetry axis, initial and final points for the homotopy path, and stop criterion.

In summary, the DBPH biparameter homotopy has the following characteristics ($a = 1$):

- Symmetry axis. It is an imaginary axis, divides the homotopy path into two symmetrical branches, right at $\lambda_{sym} = 0.5$. This is the axis where the initial and final points of the homotopy path are located.
- Initial point (λ_i). For $\lambda_1 = 0.5$ and $\lambda_2 = 0$ the solution of $H^{-1}(0)$ is known (x_i).
- Symmetrical branch 1. For $\lambda_1 = 1$ and $\lambda_2 = 1$, $H(f(x), 1, 1) = f(x)$. Means that at $\lambda_1 = 1$ and $\lambda_2 = 1$ all the solutions for $f(x)$ are located.
- Symmetrical branch 2. For $\lambda_1 = 0$ and $\lambda_2 = 1$, $H(f(x), 0, 1) = f(x)$. This means that at $\lambda_1 = 0$ and $\lambda_2 = 1$ all the solutions for $f(x)$ are located.
- Final point (x_f, λ_f). For $\lambda_1 = 0.5$ and $\lambda_2 = 0$ the solution of $H^{-1}(0)$ is known (x_f).

The homotopy (5) is a function of $n+2$ variables with n equations; n equals to the total number of nodes plus the non-NA compatible elements. Hence, it is necessary one extra equation (Roychowdhury and Melville, 1996) to use the conventional tracing techniques for homotopy paths (Vazquez-Leal et al., 2005a; Vazquez-Leal et al., 2011b; Allgower and Georg 1993). The equation is a function of λ_1 and λ_2 which will be called biparameter function $M(\lambda_1, \lambda_2) = 0$. Such equation must cross through $\lambda_i = (\lambda_1, \lambda_2) = (0.5, 0)$ and through solutions $\lambda_s = (\lambda_1, \lambda_2) = (1, 1)$. λ_i is the point where the solution of the circuit is trivial (x_i) and λ_s is the point where the solution for H is exactly the desired solution for the equilibrium equation $f(x_s) = 0$. The excursion of λ_1 starts at 0.5 because the symmetry axis has been established at $\lambda_{sym} = 0.5$. Nevertheless, intermediate points (λ_1, λ_2) of the homotopy path λ_1-λ_2 are not defined. Therefore, the following equation is proposed as the biparameter function (Vazquez-Leal et al., 2011b; Roychowdhury and Melville 2006)

$$M(\lambda_1, \lambda_2) = -\lambda_1 + \frac{\left(\lambda_2 + \dfrac{B\,(-1+A)}{AB+1-2A}\right)}{\left(-\dfrac{(-1+2\,A-B)\,\lambda_2}{AB+1-2A} + 2\,\dfrac{B\,(-1+A)}{AB+1-2A}\right)} = 0, \tag{6}$$

where $(\lambda_1, \lambda_2) = (A, B)$ is the point where the curve cross the curve of the function $M(\lambda_1, \lambda_2)$, as shown in Fig. 1(a). The value range for A and B are $[0.5, 1]$ and $[0, 1]$ respectively. For instance, in Fig. 1(b), we show a series of curves for different points (A, B), named as $p_1, p_2, ...,$ and p_{11}, obtained from (6). Following, we present the numerical results and plots for the biparameter homotopy simulation for a case study; simulations and figures were obtained using Maple 15 software.

4 Case study: circuit with bipolar transistors and a diode

A circuit with bipolar transistors and a diode was solved in Yamamura et al. (1999) and Vazquez-Leal et al. (2011a). This circuit has three operating points. The Ebers-Moll model is used for all the transistors; the equation for the model is given by

$$\begin{bmatrix} i_E \\ i_C \end{bmatrix} = \begin{bmatrix} 1 & -0.01 \\ -0.99 & 1 \end{bmatrix} \begin{bmatrix} 10^{-9}(e^{(40v_{be})} - 1) \\ 10^{-9}(e^{(40v_{bc})} - 1) \end{bmatrix},$$

where i_E represents the emitter current, i_C represents the collector current, v_{be} is the voltage drop between base and emitter, and v_{bc} is the voltage drop between base and collector.

As for the diode, the model is

$$i_d = 10^{-9}(e^{40u} - 1),$$

where u is the voltage drop between diode terminals and i_d is the current through the diode.

First, the equilibrium equation is formulated using the modified nodal analysis obtaining a system containing 14 equations and 14 variables. The circuit is shown in Fig. 2.

$$\begin{aligned}
f_1) \quad & (1.85\text{E-}3)\, v_1 - (2.5\text{E-}4)\, v_2 - (2.5\text{E-}4)\, v_6 - (1\text{E-}3)\, v_9 \\
& - (2.5\text{E-}4)\, v_{12} - (1\text{E-}4)\, v_{13} + i_E = 0, \\
f_2) \quad & - (2.5\text{E-}4)\, v_1 + (3.75\text{E-}4)\, v_2 - (1.25\text{E-}4)\, v_5 + (9.9\text{E-}9) \exp(40\, v_4 - 40\, v_3) + 1\text{E-}10 \\
& - (1\text{E-}8) \exp(40\, v_4 - 40\, v_2) = 0, \\
f_3) \quad & (1\text{E-}2)\, v_3 - (1\text{E-}8) \exp(40\, v_4 - 40\, v_3) + 9.9\text{E-}9 \\
& + (1\text{E-}10) \exp(40\, v_4 - 40\, v_2) = 0, \\
f_4) \quad & (1.25\text{E-}4)\, v_4 - (1.25\text{E-}4)\, v_6 + (1\text{E-}10) \exp(40\, v_4 - 40\, v_3) - 1\text{E-}8 \\
& + (9.9\text{E-}9) \exp(40\, v_4 - 40\, v_2) = 0, \\
f_5) \quad & - (1.25\text{E-}4)\, v_2 + (1.25\text{E-}4)\, v_5 + (1\text{E-}10) \exp(40\, v_5 - 40\, v_7) - 1\text{E-}8 \\
& + (9\text{E-}9) \exp(40\, v_5 - 40\, v_6) = 0, \\
f_6) \quad & - (2.5\text{E-}4)\, v_1 - (1.25\text{E-}4)\, v_4 + (3.75\text{E-}4)\, v_6 + (9.9\text{E-}9) \exp(40\, v_5 - 40\, v_7) + 1.01\text{E-}8 \\
& - (1\text{E-}8) \exp(40\, v_5 - 40\, v_6) - (1\text{E-}8) \exp(40\, v_8 - 40\, v_6) = 0, \\
f_7) \quad & (1\text{E-}2)\, v_7 - (1\text{E-}8) \exp(40\, v_5 - 40\, v_7) + 9.9\text{E-}9 + (1\text{E-}10) \exp(40\, v_5 - 40\, v_6) = 0, \qquad (7) \\
f_8) \quad & (30\text{E}3)^{-1}\, v_8 - (30\text{E}3)^{-1}\, v_9 + (1\text{E-}8) \exp(40\, v_8 - 40\, v_6) - 1\text{E-}8 = 0, \\
f_9) \quad & - (1\text{E-}3)\, v_1 - (30\text{E}3)^{-1}\, v_8 + (31)\, (30\text{E}3)^{-1}\, v_9 + (9.9\text{E-}9) \exp(40\, v_{11} - 40\, v_{10}) + 1\text{E-}10 \\
& - (1\text{E-}8) \exp(40\, v_{11} - 40\, v_9) = 0, \\
f_{10}) \quad & (1\text{E-}2)\, v_{10} - (1\text{E-}8) \exp(40\, v_{11} - 40\, v_{10}) + (9.9\text{E-}9) + 1\text{E-}10 \exp(40\, v_{11} - 40\, v_9) = 0, \\
f_{11}) \quad & (1\text{E-}4)\, v_{11} - (1\text{E-}4)\, v_{12} + (1\text{E-}10) \exp(40\, v_{11} - 40\, v_{10}) - 1\text{E-}8 \\
& + (9.9\text{E-}9) \exp(40\, v_{11} - 40\, v_9) = 0, \\
f_{12}) \quad & - (2.5\text{E-}4)\, v_1 - (1\text{E-}4)\, v_{11} + (3.5\text{E-}4)\, v_{12} + (9.9\text{E-}9) \exp(40\, v_{13}) + 1\text{E-}10 \\
& - (1\text{E-}8) \exp(40\, v_{13} - 40\, v_{12}) = 0, \\
f_{13}) \quad & - (1\text{E-}4)\, v_1 + (1.1\text{E-}3)\, v_{13} + (1\text{E-}10) \exp(40\, v_{13}) - 1\text{E-}8 \\
& + (9.9\text{E-}9) \exp(40\, v_{13} - 40\, v_{12}) = 0, \\
f_{14}) \quad & v_1 - 12 = 0.
\end{aligned}$$

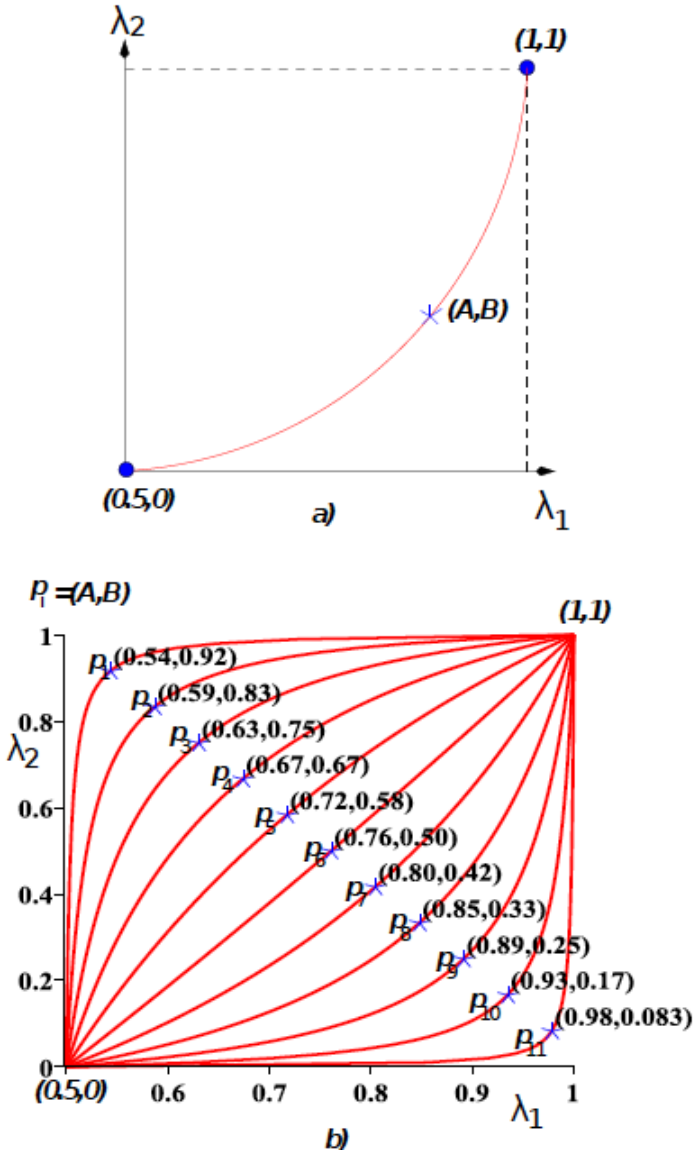

Figure 1: Path of $M(\lambda_1, \lambda_2) = 0$ for different points $p = (A, B)$.

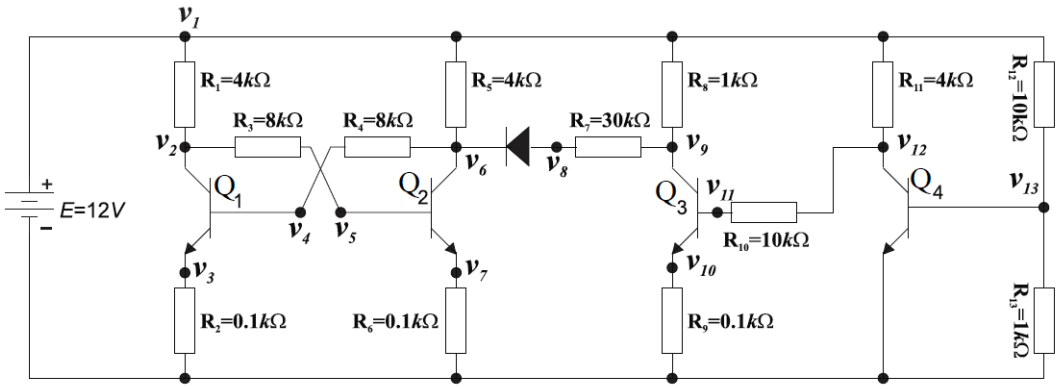

Figure 2: Circuit with bipolar transistors and a diode.

Now, DBPH homotopy is applied to solve the circuit; the homotopy formulation is expressed as follows ($a = 1$, $C = 1$)

$$\begin{aligned}
H_1) &\quad (\lambda_1+1)\lambda_1(\lambda_1-1)(\lambda_1-2)(v_1-13)(v_1+13)+(\lambda_1-0.5)^2 f_1^2=0,\\
H_2) &\quad (\lambda_1+1)\lambda_1(\lambda_1-1)(\lambda_1-2)(v_2-13)(v_2+13)+(\lambda_1-0.5)^2 f_2^2=0,\\
&\quad\quad\vdots\\
H_{13}) &\quad (\lambda_1+1)\lambda_1(\lambda_1-1)(\lambda_1-2)(v_{13}-13)(v_{13}+13)+(\lambda_1-0.5)^2 f_{13}^2=0,\\
H_{14}) &\quad (\lambda_1+1)\lambda_1(\lambda_1-1)(\lambda_1-2)(I_E-13)(I_E+13)+(\lambda_1-0.5)^2 f_{14}^2=0,\\
M) &\quad M(\lambda_1,\lambda_2)=0.
\end{aligned} \tag{8}$$

In order to show the effects for specifically selecting a biparameter function $M(\lambda_1, \lambda_2) = 0$, four particular cases were chosen (see Fig. 1(b) for p_1, p_6, and p_{11} biparameter paths).

1. M_1 path associated to point p_1 (see Fig. 3(a) and Fig. 3(b)). This path is an extreme case of biparameter functions, which is qualitatively characterized, first by the, λ_2 parameter from 0.0 until 1 and subsequently deforms λ_1 from 0.5 until 1.
2. M_6 path associated to point p_6 (see Fig. 3(c) and Fig. 3(d)). This path represents the case where homotopy parameters keep an approximate linear aspect ratio.
3. M_{11} path associated to point p_{11} (see Fig. 3(e) and Fig. 3(f)). This path is an extreme case of biparameter function; it is characterized by deforming first the λ_1 parameter from 0.5 until 1 and subsequently distorts λ_2 from 0.0 until 1.
4. M_{12} path (see Fig. 4(b) and Fig. 4(c)). In Fig. 4(a) a case of third order polynomial biparameter function is shown.

Table 1 summarize the results for tracing (Vazquez-Leal et al., 2005a) all four homotopy paths; each one with a different biparameter function but having the same initial point. Then, the results are:

- All four paths showed double bounding and symmetry axis $\lambda_{sym} = 0.5$.
- The corresponding symmetrical branch was traced successfully ($\lambda_1 = 1$ and $\lambda_2 = 1$).
- For every case all three operating points were located (see Table 1).

R.P.	Iter	TP	v_1	v_2	v_3	v_4	v_5	v_6	v_7
x_i	-	-	$+13$	$+13$	$+13$	-13	$+13$	$+13$	$+13$
S_1	-	-	12	5.995	0.085	0.368	0.712	0.436	0.390
S_2	-	-	12	0.883	0.278	0.590	0.631	0.812	0.315
S_3	-	-	12	0.405	0.366	0.6854	0.349	6.796	0.070
$x_f(M_1)$	16669	11	$+13$	$+13$	$+13$	-13	$+13$	$+13$	$+13$
$x_f(M_6)$	17063	11	$+13$	-13	$+13$	-13	$+13$	$+13$	$+13$
$x_f(M_{11})$	16508	11	$+13$	$+13$	$+13$	-13	$+13$	$+13$	$+13$
$x_f(M_{12})$	16112	11	$+13$	$+13$	-13	-13	$+13$	$+13$	$+13$

R.P.	Iter	TP	v_8	v_9	v_{10}	v_{11}	v_{12}	v_{13}	i_E
x_i	-	-	$+13$	$+13$	$+13$	$+13$	$+13$	-13	-13
S_1	-	-	0.699	11.635	0.4E-5	0.039	0.039	0.321	-0.0089
S_2	-	-	1.074	11.647	0.4E-5	0.039	0.039	0.321	-0.0100
S_3	-	-	7.038	11.839	0.4E-5	0.039	0.039	0.321	-0.0085
$x_f(M_1)$	16669	11	$+13$	$+13$	$+13$	$+13$	$+13$	-13	$+13$
$x_f(M_6)$	17063	11	$+13$	$+13$	$+13$	$+13$	$+13$	-13	$+13$
$x_f(M_{11})$	16508	11	$+13$	$+13$	$+13$	$+13$	$+13$	-13	$+13$
$x_f(M_{12})$	16112	11	$+13$	$+13$	$+13$	$+13$	$+13$	-13	$+13$

Table 1: Relevant points and solutions considering $\lambda_1 = 0.5$ and $\lambda_2 = 0$ at the symmetry axis and $\lambda_1 = 1$ and $\lambda_2 = 1$ at solution (S_1, S_2 and S_3).

- The number of turning points (TP) is eleven for all four paths.
- The final point for paths M_1 and M_{11} is the same. This implies that extreme paths may be similar no matter which parameter is swept first (λ_1 or λ_2).
- The final point for path M_6 and M_{12} differs from the other paths (M_1 and M_{11}). This result implies that it is possible to affect the homotopy path depending on the selection made for the biparameter function M.
- A polynomial biparameter function (M_{12}) was implemented as

$$M_{12}(\lambda_1, \lambda_2) = -\lambda_2 + 98.095238\lambda_1^3 - 221\lambda_1^2 + 161.83333\lambda_1 - 37.928571 = 0. \quad (9)$$

The biparameter function M_{12} contains two critical points while the other three paths M_1, M_6, and M_{12} show a simple behaviour of being monotonically increasing. In this respect, it can be said that M_{12} possess higher nonlinearity than the rest of the biparameter functions used.

For the biparameter function M_{12}, the total number of iterations (Iter=16112) were lower than the iterations reached using biparameter functions: M_1, M_6, and M_{11}; even the final point of the path is different compared to the rest of the paths. Therefore, the selection of the biparameter function plays an important role on the performance of the biparameter DBPH homotopy. In fact, for this case study, the selection of the most nonlinear biparameter function generated the least number of iterations.

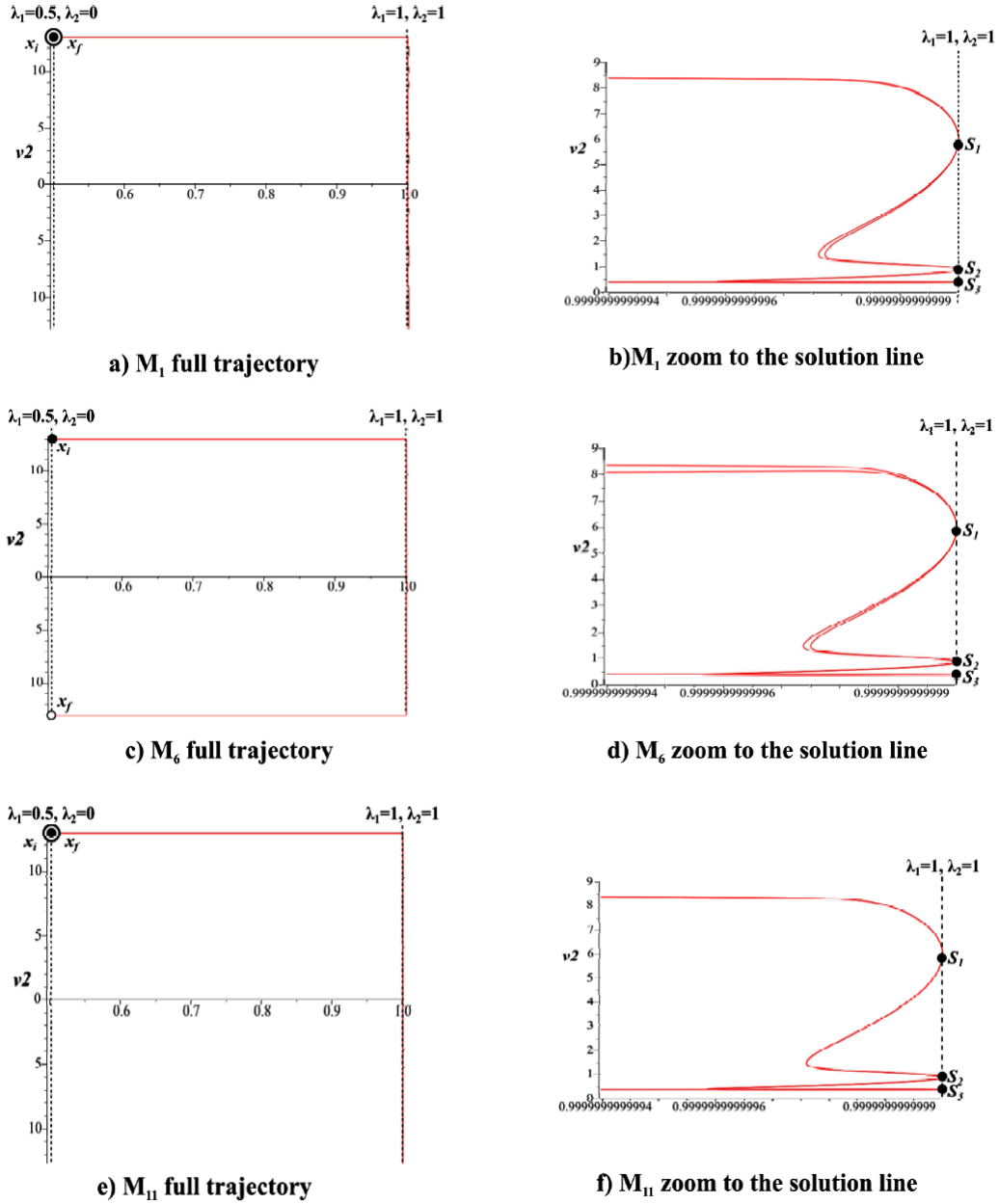

Figure 3: Homotopy path for $v_2 - \lambda_1$ using biparameter function: a) M_1, b) zoom to M_1, c) M_6, d) zoom to M_6, e) M_{11}, f) zoom to M_{11}. For all cases the zoom factor for λ_1 is $8.33\text{E}11$.

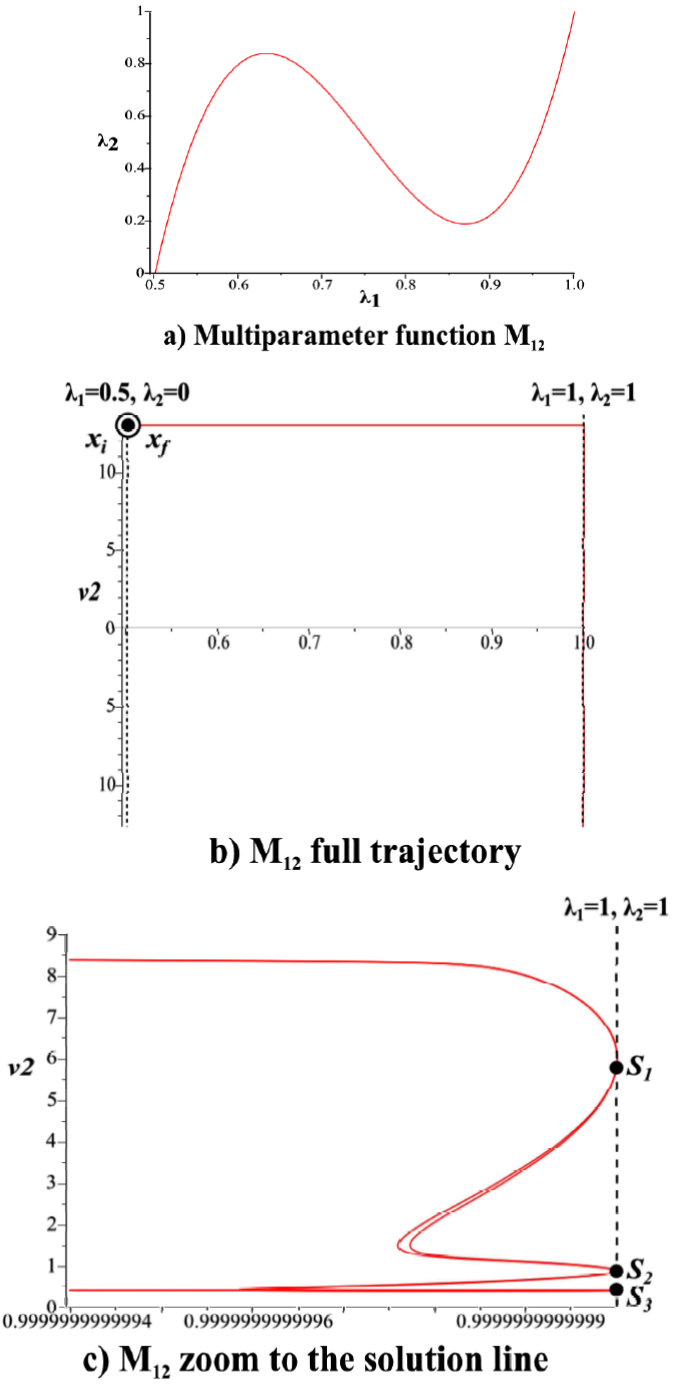

Figure 4: a) Biparameter function M_{12}, b) Homotopy path for $v_2 - \lambda_1$ using biparameter function M_{12} and c) Zoom to solution line with a factor $8.33\text{E}11$ for λ_1.

5 Discussion

All paths in Table 1 have the same number of solutions and turning points but different number of iterations; it means that all paths could have similar aspects as shown in Fig. 3 and Fig. 4. Also, despite that M_6 shows the most "linear" behaviour from all the employed biparameter functions, this function generates the path with the highest number of iterations and different final point (compared to M_1, M_{11}, and M_{12}); meaning that it is possible to affect the homotopy path with an appropriate selection of M. For the case study, fewer number of iterations were achieved using the most nonlinear biparameter function (M_{12}); therefore, a nonlinear biparameter function M may exist creating an optimized homotopy path. Hence, future research should focus in establishing rules to formulate a biparameter function M allowing the optimization of the homotopy path in aspects like: length, sharp points, among others. Last, multiplying λ_2 by the stimulus vector i_{est} helps to decrease the nonlinear effects of the equilibrium equation and increase the probability to locate one or more solutions.

The proposed homotopy locates multiple operating points, possesses automatic stop criterion, symmetry, and solution lines; contrary to the multiparameter homotopy shown in Roychowdhury and Melville (1996), which does not possess any of the characteristics mentioned above. Nevertheless, in Roychowdhury and Melville (1996), circuit simulations containing up to 8489 MOS transistors were shown, that it is important for industrial purposes. Also, one of the main challenges for applying the biparameter DBPH homotopy in circuit simulation of VLSI MOS circuits will be the selection of a unified low complexity mathematical model for the MOS transistor for DC (Jen at al., 1997; Jen, 1998; Ramaswamy et al., 1997; Zhou et al., 2011), which enables performing fast and accurate simulations. Therefore, in a future work, we will test the DBPH homotopy solving the equilibrium equation of VLSI MOS circuits.

6 Conclusion

This work has shown a biparameter DBPH homotopy with formal stop criterion. Also, we established that is feasible to affect the homotopy path by selecting different biparameter functions; likewise, different homotopy simulations for the same circuit, showed that by selecting the same initial point and different biparameter functions gave as result that, for the most nonlinear function, we obtained the lowest number of iterations to complete the tracing of a symmetrical branch. Therefore, the selection of the biparameter function can affect the homotopy path. Nevertheless, further study is required including tests with larger circuits and other types of biparameter functions to establish selection criteria for the biparameter function that generates an optimized homotopy path.

Acknowledgment

The authors wish to acknowledge to Rogelio-Alejandro Callejas-Molina and Roberto Ruiz-Gomez for their technical support. Besides, this work has been supported by CONACYT México research project CB-2010-01 #157024.

Competing interests

The authors declare that they have no competing interests.

References

Allgower, E.L., Georg, K. (1993). Continuation and path following. Acta Numerica, 2, 1–64.

Di Rocco, S., Eklund, D., Peterson, C., Sommese, A.J. (2011). Chern numbers of smooth varieties via homotopy continuation and intersection theory. Journal of Symbolic Computation, 46(1), 23–33.

Goldgeisser, L.B., Green, M.M. (1998). A novel algorithm that finds multiple operating points of nonlinear circuits automatically. In: Proceedings of the 1998 IEEE International Symposium on Circuits and Systems, Monterey, USA: May 3–June 3.

Goldgeisser, L.B., Green, M.M. (2005). A Method for Automatically finding Multiple Operating Points in Nonlinear Circuits. IEEE transactions on circuits and systems-I: fundamental theory and aplications, 52(4), 776–784.

Ho, C-W., Ruehli, A., Brennan, P. (1975). The modified nodal approach to network analysis. IEEE Transactions on Circuits and Systems, 22(6), 504–509.

Jalali, F., Seader, J.D., Khaleghi, S. (2008). Global solution approaches in equilibrium and stability analysis using homotopy continuation in the complex domain. Computers & Chemical Engineering, 32(10), 2333–2345.

Jen, S.H., Sheu, B.J., Oshima, Y. (1997). A Unified Approach to Submicron DC MOS Transistor Modeling for Low-Voltage ICs. Analog Integrated Circuits and Signal Processing, 12(2), 107–118.

Jen, S.H. (1998). A compact and unified MOS DC current model with highly continuous conductances for low-voltage ICs. IEEE Transactions on Computer-Aided Design of Integrated Circuits and Systems, 17(2), 169–172.

Kuroki, W., Yamamura, K., Furuki, S. (2007). An efficient variable gain homotopy method using the SPICE-oriented approach. IEEE Transactions on Circuits and Systems-II: Express Briefs, 54(7), 621–625.

Lagarias, J.C., Trajković, L. (1999). Bounds for the Number of DC Operating Points of Transistor Circuits. IEEE Transactions on Circuits and Systems-I: Fundamental Theory and Applications, 46(10), 1216–1221.

Ma, W., Trajkovic, L., Mayaram, K. (2002). HomSSPICE: a homotopy-based circuit simulator for periodic steady-state analysis of oscillators. In: Proceedings IEEE International Symposium on Circuits and Systems, Scottsdale, USA: May 26–29.

Malinen, I., Tanskanen, J. (2010). Homotopy parameter bounding in increasing the robustness of homotopy continuation methods in multiplicity studies. Computers & Chemical Engineering, 34(11), 1761–1774.

Ogrodzki, J. (1994). Circuit simulation: methods and algorithms. CRC Press Inc.

Ramaswamy, S., Amerasekera, A., Chang, M.-C. (1997). A unified substrate current model for weak and strong impact ionization in sub-0.25 m NMOS devices. In: Electron Devices Meeting, Dallas, USA: December 7–10.

Roychowdhury, J., Melville, R. (1996). Homotopy techniques for obtaining a DC solution of large-scale MOS Circuits. In: Proceedings 33rd Design Automation Conference, Las Vegas, USA: June 3–7.

Roychowdhury, J., Melville, R. (2006). Delivering global DC convergence for large mixed-signal circuits via homotopy/continuation methods. IEEE Transactions on Computer-Aided Design of Integrated Circuits and Systems, 25(1), 66–78.

Sarmiento-Reyes, A., Murphy-Arteaga, R.S., Vazquez-Leal, H. (2001). A MAPLE-based homotopic circuit simulation package. In: Proceedings of the 44th IEEE Midwest Symposium on Circuits and Systems, Dayton, USA: August 14–17.

Varedi, S.M., Daniali, H.M., Ganji, D.D. (2009). Kinematics of an offset 3-UPU translational parallel manipulator by the homotopy continuation method. Nonlinear Analysis: Real World Applications, 10(3), 1767–1774.

Vazquez-Leal, H., Hernandez-Martinez, L., Sarmiento-Reyes, A., Castaneda-Sheissa, R. (2005). Numerical continuation scheme for tracing the double bounded homotopy for analysing nonlinear circuits. In: Proceedings 2005 International Conference on Communications, Circuits and Systems, Hong Kong, China: May 27–30.

Vazquez-Leal, H., Hernandez-Martinez, L., Sarmiento-Reyes, A. (2005). Double-Bounded Homotopy for analysing nonlinear resistive circuits. In: Proceedings IEEE International Symposium on Circuits and Systems, Kobe, Japan: May 23–26.

Vazquez-Leal, H., Hernandez-Martinez, L., Sarmiento-Reyes, A., Castaneda-Sheissa, R., Gallardo-Del-Angel, A. (2011). Homotopy method with a formal stop criterion applied to circuit simulation. IEICE Electronics Express, 8(21), 1808–1815.

Vazquez-Leal, H., Castaneda-Sheissa, R., Rabago-Bernal, F., Hernandez-Martinez, L., Sarmiento-Reyes, A., Filobello-Nino, U. (2011). Powering multiparameter homotopy-based simulation with a fast path-following technique. ISRN Applied Mathematics, 2011(Article ID 610637), 7 pages.

Verhoeven, C.J.M., van Staveren, A., Monna, G.L.E., Kouwenhoven, M.H.L., Yildiz, E. (2003). Structured electronic design: negative-feedback amplifiers. Dordrecht: Kluwer Academic Publishers.

Wolf, D.M., Sanders, S.R. (1996). Multiparameter Homotopy Methods for finding DC operating points of Nonlinear Circuits. IEEE Transactions on Circuits and Systems-I: Fundamental Theory and Applications, 43(10), 824–837.

Wu, T.-M. (2005). A study of convergence on the Newton-homotopy continuation method. Applied Mathematics and Computation, 168(2), 1169–1174.

Wu, T.-M. (2006). Solving the nonlinear equations by the Newton-homotopy continuation method with adjustable auxiliary homotopy function. Applied Mathematics and Computation, 173(1), 383–388.

Wu, T.-M. (2006). The inverse kinematics problem of spatial 4P3R robot manipulator by the homotopy continuation method with an adjustable auxiliary homotopy function. Nonlinear Analysis: Theory, Methods & Applications, 64(10), 2373–2380.

Yamamura, K., Sekiguchi, T., Inuoe, Y. (1999). A fixed-point homotopy method for solving modified nodal equations. IEEE Transactions on Circuits and Systems-I: Fundamental Theory and Applications, 46(6), 654–664.

Zhou, X., Zhu, G., See, G.H., Chandrasekaran, K., Chiah, S.B., Lim, K.Y. (2011). Unification of MOS compact models with the unified regional modeling approach. Journal of Computational Electronics, 10(1–2), 121–135.